

# The Sky's the Limit

FOCUSED  
ISSUE FEATURE



PHOTO COURTESY OF ORBITAL SCIENCES

*Rudy Emrick, Pedro Cruz, Nuno B. Carvalho,  
Steven Gao, Rüdiger Quay, and Patrick Waltereit*

**T**he growth of demand for broadband has been seen in satellite communications as it has in other aspects of the market. Satellites carry media content around the globe, which includes satellite television, radio, and broadband services directly to consumers.

Satellite communications also allows for mobile or nomadic voice and data globally. They are also critical to disaster recovery and emergency preparedness, providing critical communications following natural disasters. While the sole application of some satellites is the distribution of data, all satellites require

---

*Rudy Emrick (rudymerrick@ieee.org) is with Orbital Sciences, Phoenix, Arizona, United States. Pedro Cruz (pcruz@av.it.pt) and Nuno B. Carvalho (nbcarvalho@ua.pt) are with the Instituto de Telecomunicações DETI, Universidade de Aveiro, Portugal. Steven Gao (s.gao@kent.ac.uk) is with the University of Kent, United Kingdom. Rüdiger Quay (Ruediger.Quay@iaf.fraunhofer.de) and Patrick Waltereit are with the Fraunhofer Institute of Applied Solid-State Physics.*

Digital Object Identifier 10.1109/MMM.2013.2296212  
Date of publication: 7 March 2014

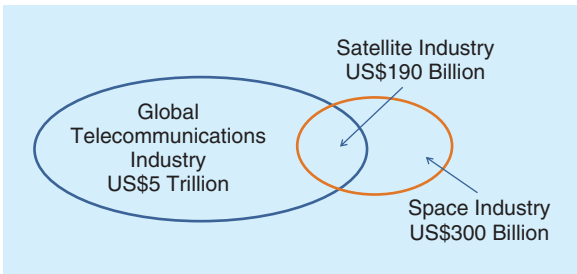


**Figure 1.** Relative market sizes of the telecommunications, space, and the satellite industries [1].

communication systems technology. For example, remote sensing satellites may be collecting environmental data, but the data collected and the command and control of the satellite both rely on communication technology. If large amounts of data is being collected, broadband data links are required to avoid loss of data since on-board storage capacity for this data is limited.

### Satellite Market

While the satellite industry is a relatively small percentage of the overall telecommunications industry, it's still a large market in terms of dollars. As shown in Figure 1, the overall telecommunications industry is on the order of US\$5 trillion and the space industry is on the order of US\$300 billion. The satellite industry, which is on the order of US\$190 billion, is a subset of both the telecommunications and space industries, representing about 60% of the space industry and 4% of the global telecommunications industry. [1]–[4]

A breakout of the types of satellites currently in orbit is shown in Figure 2. The vast majority of satellites are in either low-earth-orbit or geosynchronous orbit. Looking at the functions of those currently in orbit, about 38% are commercial communications satellites with an additional 20% dedicated to civil government or military communications, making communications the most common function of satellites launched. As mentioned earlier, even those with a primary function other than communications must still leverage communications technology.

Communications satellites are moving toward the realization of true high-throughput satellites (HTS), which can offer 2–20 times the total throughput of typical fixed satellite service that is offered today. The Internet protocol (IP) over satellite market is pushing this trend, and the move toward true HTS will allow the cost per megabyte to continue downward. In addition, there is also a great market potential for narrow-band machine-to-machine (MTM) applications as the costs in delivering data continue downward. These applications, and the combinations of them, add to the need for operators to have greater ability to dynamically allocate bandwidth and efficiently use their available spectrum.

As with all markets, it can be difficult to predict the future very far out in time. One of the challenges in deploy-

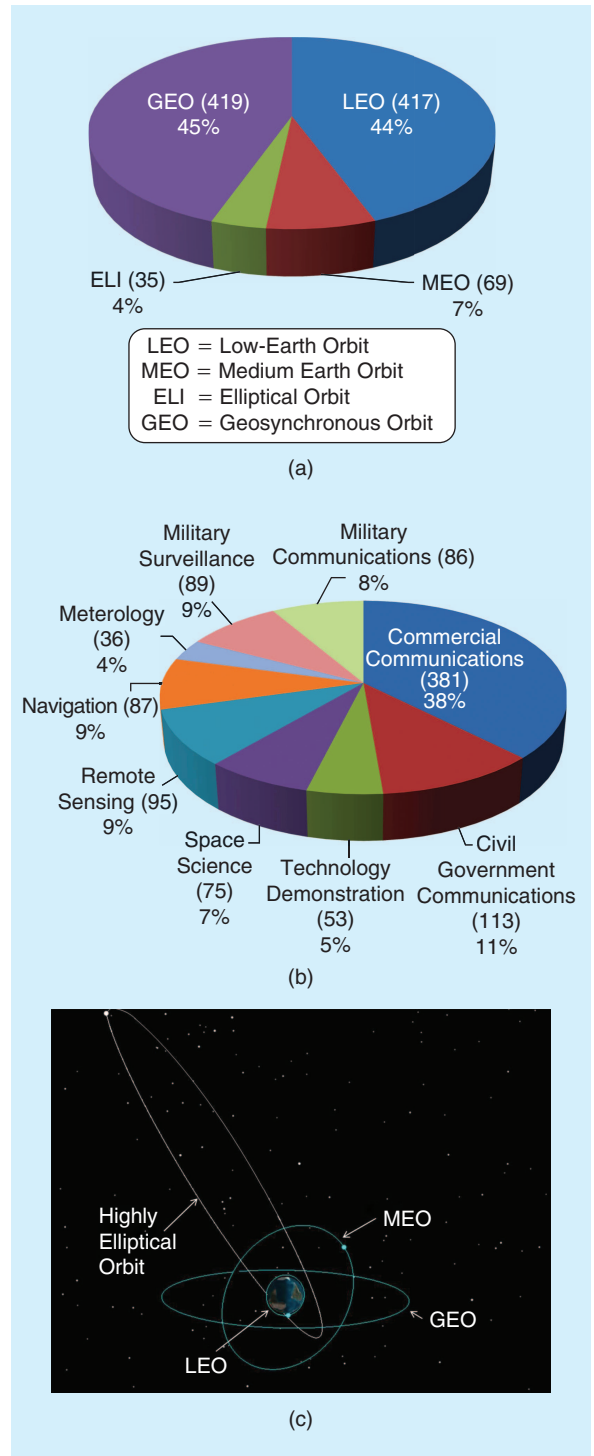


**Figure 2.** A breakout of operational satellites by orbit and function (from [1]). (a) Operational satellites by orbit, (b) operational satellites by function, and (c) a representation of satellite orbit types.

ing communications satellites is having a design that will remain aligned with the needs of your customer base over the lifetime of the satellite. A typical design life for a geostationary satellite is 15 years, while market projections are difficult if not impossible to be accurate for more than a few years into the future. It's this challenge that is one of

the drivers in defining the key microwave technologies that are a focus for satellite communications. Key system focus areas are delivering larger overall bandwidths and having the ability to allocate more or less bandwidth over regions as the demand from your customer base changes. The ability to adapt when another satellite is added to the fleet, so that those combinations of older and newer satellites can be adapted to bandwidth demands across the region of end users is also important.

### Communications Satellite Architecture

A typical communications satellite system architecture is shown in Figure 3. The system will include a gateway that serves as the satellite's space-to-ground interface with the service provider. Within the gateway, the service provider may have a range of interfaces to the core Internet or other data content that's being provided to the end users. The satellite will have a gateway spot beam, which is a directive antenna pointed at the gateway ground station. This communications link must be able to handle the full aggregate data, up and down, to all end users. As an example, ViaSat-1, which was launched in 2012, has a total throughput capacity of 134 Gb/s [3]. On board the satellite, the channels to each end user are provided through a series of spot beams. By using spot beams, the frequency bands allocated to this satellite can be reused across large geographical areas. Polarization can also be used across multiple beams to enable greater spectral efficiency and reuse.

An example of how multiple beams may be used to maximize reuse and coverage is shown in Figure 4. A multibeam antenna allows for band reuse which is dependent on the antenna performance, where each beam is a separate channel. A portion of the operating bandwidth is assigned to each channel. Each channel (beam) covers a unique geographic area. In Figure 4, a color is assigned to each channel and polarization sense combination. In a four-color plan, half of the total bandwidth is allocated to each polarization sense and one quarter of total bandwidth is allocated for each channel. Each beam is a single channel/polarization and color. Isolation is achieved through a combination of polarization discrimination, spatial diversity and frequency separation. In this example, there is always one noninterfering beam between each set of beams that could interfere with each other. Using architectures like this can enable much higher throughputs to each end user. In addition, the service provider may

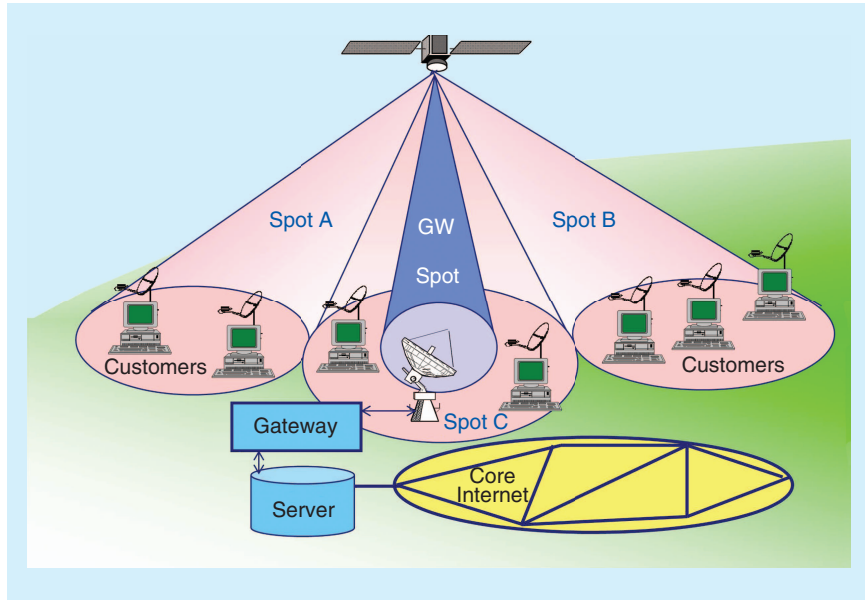


Figure 3. Typical communications satellite system architecture [6].

also reallocate the total available throughput across the region to meet changing demand. For example, the rate limits may be increased in the western United States to meet early evening increased demands while reducing the rate limits in the east since it is in a time zone that is three hours later and demand there may have already tapered off for the day. Ideally, the service provider would like to fully utilize the total throughput of the satellite as much of the time as possible.

To improve the ability to provide greater bandwidths along with the ability to adapt coverage areas and allocation of bandwidth across regions over time, key technologies include channelization technology, GaN, moving beyond Ka-band to enable larger available bandwidths,

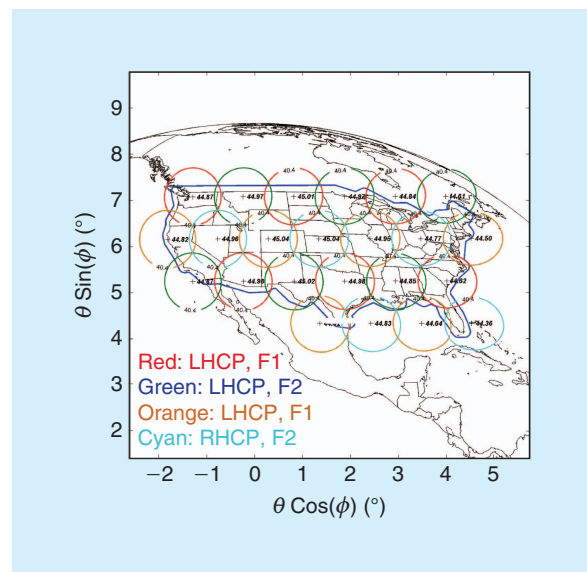


Figure 4. An example four-color plan for frequency reuse [6], [8].

**It is expected that the Gateway links will be first to move to higher bands that are beyond Ka-band, since these links must be able to handle the full data capacity of the satellite.**

adaptive and steerable antennas for space and software-defined radios (SDRs). Each of these contributes to enabling the use of existing bandwidth more efficiently, increasing total available bandwidth or both.

### Channelizer

The channelizer is used to distribute the total data capacity of the satellite across all of the beams it has for distribution. Ideally, the channelizer will also allow the satellite operator to move bandwidth from one beam to another. This will allow the operator to provide backhaul data to, for example, a remote ski area on weekends when demand is high and move that capacity elsewhere to meet those demands during different times of the week or year [8], [9]. The channelizer functionality may be integrated with a SDR, since each can be software defined and reconfigurable. An example payload block diagram is shown in Figure 5. The channelizer is central to the management of the satellite

throughput and how it is distributed among the beams that form its coverage area.

### GaN for Space Applications

Providing sufficient isotropic radiated power with sufficient link margin is important for wireless telecommunications with high availability. One of the key elements of the RF front is the power amplifier (PA). GaN HEMTs have demonstrated ability for realizing high performance in high-PAs (HPA). As GaN continues to mature, it is being considered for applications where mature technology and reliability are key, which includes space. It is well known that GaN devices can offer higher efficiencies and can operate at higher voltages compared with GaAs HEMT or LDMOS [11], [12]. They provide significant advantages in linear output power, system efficiency, bandwidth, and overall compactness [14]–[16]. In space applications, the vacuum electronic based traveling wave tube amplifier (TWTA) is still used because of their high efficiency. One drawback of the TWTA is the need for extremely high voltages, which are on the order of several thousands of volts. With these high voltages, some suggest that reliability is not ideal [12] while others indicate the TWTA reliability may be better than solid-state PAs (SSPAs) [13]. TWTAs may require more mass and volume compared to solid-state solutions. The SSPA is often considered a favorable

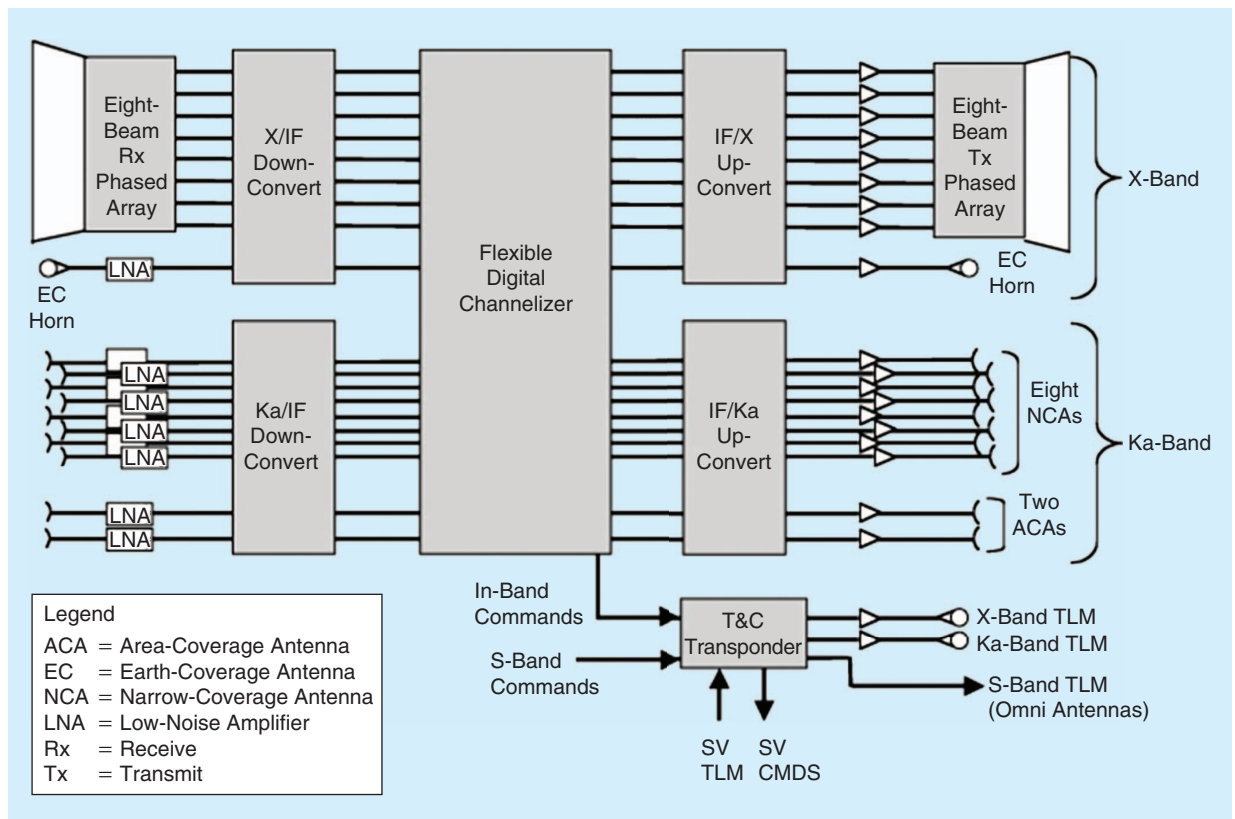


**Figure 5.** A payload block diagram that includes a flexible digital channelizer. The channelizer enables adaptive distribution of the satellites total data capacity across the satellites coverage area(s) which typically include multiple spot beams (from [10] with permission from Boeing).

solution and the performance demonstrated by GaN devices shows what many believe is the real potential for solid-state amplifiers to replace TWTAs. In this context, direct tube replacement by solid-state devices poses a great challenge in the tradeoff between linearity and efficiency. GaN-based SSPAs may offer several advantages in terms of cost, volume, and weight, in addition to overall availability over the lifetime of the system. With these potential advantages, linear efficiency and gain are key in the advancement of this technology, as any solid-state solution, specifically at frequencies beyond C-band, and will be inferior to tubes on the device level. The choice of the superior solution, TWTAs or SSPAs, is not without debate. It is likely that the choice between a TWTAs and a SSPA for a given system will depend on the specific requirements for that system which include frequency of operation, output power, efficiency, linearity, mass, volume, and reliability. At the same time, new antenna approaches, which are discussed later, may offer the real drive in moving toward solid-state amplifiers. Active multifeed, multibeam antennas may require a relatively large number of PAs to generate the overall output power by active beamforming. For this to happen, GaN devices will need to be demonstrated to have this performance and reliability in real space environments to gain true acceptance within the space industry. The demonstration of performance and reliability in space environments is ongoing and can take some time to complete, since the technology must find opportunities within satellites being deployed and gain the time on orbit to demonstrate robustness.

As one example for an actual GaN monolithic microwave integrated circuit (MMIC) deployment in space,

## The continued increased demand for broadband data continues across the full telecommunications industry which includes satellite communications.

Figure 6 shows a dual-stage GaN MMIC for a frequency range around 8 GHz. It provides an output power of up to 8 W in CW-operation with more than 25-dB gain and with a power-added efficiency (PAE) around 45%. Reliability and initial space radiation tests were found to be very promising, e.g., [17] and [19]. The MMIC was then integrated and spaceborn in May 2013 along with the European Space Agency (ESA) Proba-V mission [19] to serve a technology demonstrator in the telemetry link. Even more efficient versions of this MMIC are now available, which provide efficiencies PAE beyond 50%.

Given the small footprint, similar GaN MMICs will be extremely useful for integration into future active multibeam systems. In addition to high power applications, GaN devices may also offer solutions for low noise gain blocks which are also key for communication system implementations [20], [21].

### Moving Beyond Ka-Band

To continue meeting the demand for increasing bandwidth, satellite operators continue to move up in frequency where there is more available bandwidth, just as portions of the telecommunications market has. Today, satellites are being deployed that leverage Ka-band frequencies. It is expected that the Gateway links will be

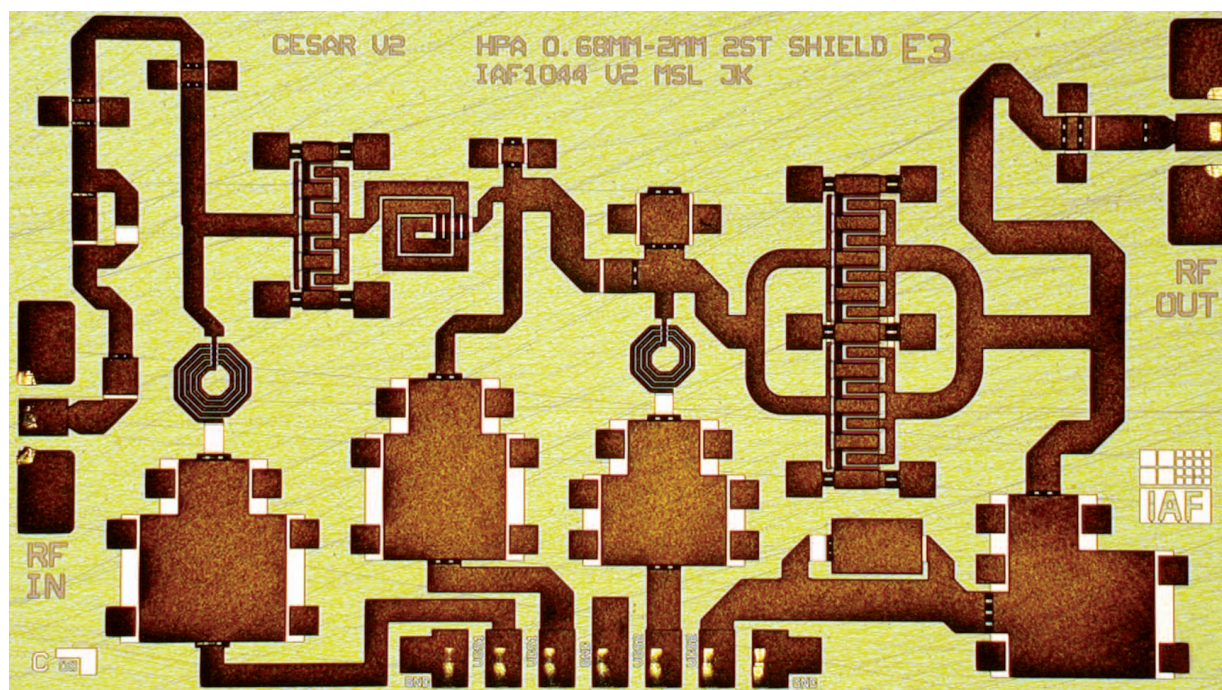
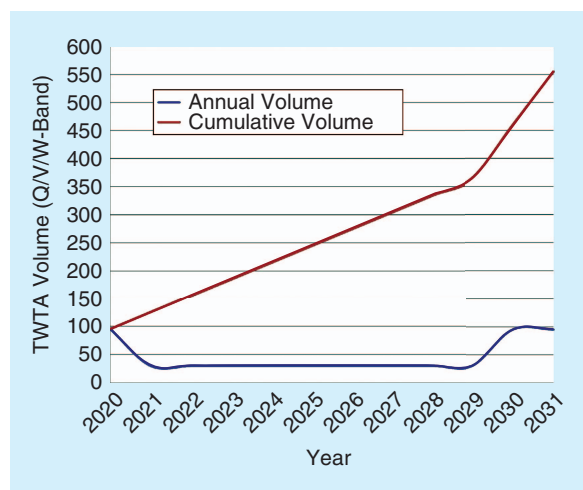


Figure 6. Dual-stage X-band GaN MMIC (size: 3.5 mm × 2 mm) from [16].

## Software defined radio and cognitive radio are the technologies that promise more efficient approaches to truly generalized radios that are able to use whichever communications waveforms one desires.

first to move to higher bands that are beyond Ka-band, since these links must be able to handle the full data capacity of the satellite. To move to higher frequency bands, some key areas must be addressed. These areas include the availability of mature, reliable, RF front-end components along with a true understanding of the channel characteristics. Some work has been done in looking at moving beyond Ka-band, but too many questions remain [22], [23]. To move to higher bands, key channel characteristics like rain attenuation, the effects of clouds versus clear air, polarization changes, and dynamic effects like fade duration and fade rates must be understood. To fully characterize the channel and understand these unknowns, a measurement payload is in development to provide a stable and constant measurement system over a prolonged period. Recently, the U.S. Air Force Research Laboratory (AFRL) published a call for proposals to develop a W/V-band communications experiment and awarded a phase 1 [24]. Two experiment types were identified, which include a beacon and a transponder [25]. Beacons are planned for V (71–76 GHz) and W (81–86 GHz) bands. Transponders will provide active data transmission and have the capability to demonstrate multiple high-data-rate channels. The experiment is being developed so that it can be a hosted payload, which should allow for faster deployment at a lower cost.

Along with understanding the channels above Ka-band, RF front-end component availability is also



**Figure 7.** Estimated TWTA market. First deployments for Gateway links are expected in the early 2020s with the band becoming a common selection about ten years later [6], [7].

fundamental. As discussed earlier, GaN shows great promise and may be a real solution for these higher bands. The alternative to using GaN of high power is the continued use of TWTAs, which are widely used today in space, though not at frequencies above Ka-band. TWTAs operating in Q/V/W band must be qualified for space applications. Historically, TWTAs are typically qualified before solid-state solutions. While it is not expected that real volumes will need to be available until around 2020 [6], the cumulative volumes are expected to begin increasing shortly after with a substantial rise about ten years later, as shown in Figure 7. It is important to keep in mind that the product design cycles in the space industry move at a much different pace than those in, for example, consumers electronics. This is due largely to both the cost of building and deploying a satellite along with the long design life of each (around 15 years).

### Adaptive and Steerable Antennas for Space

To communicate with small mobile terminals on the ground, high equivalent isotropic radiated power (EIRP) and gain/noise temperature ratio (G/T) are required. The antenna system onboard the satellite needs to have high gain, multiple spot beams, and beam-steering capabilities [27]. The antenna must also be tailored for optimum efficiency and power handling. The polarization can be left-hand and right-hand circularly polarized for transmit and receive, respectively, while linear polarizations are also used in some satellites.

Many antennas have been developed, including the conventional parabolic antenna, shaped reflector antenna, the direct radiating phased-array antenna, the phased-array-fed single reflector antenna, the phased-array-fed imaging reflector antenna, printed reflectarray, lens, and horn [27].

### Phased-Array Antennas

A high-rate downlink has been traditionally accomplished employing a high gain reflector antenna. A direct radiating phased-array antenna offers several advantages over reflector antennas in this application: A phased-array antenna can achieve electronic beam steering, thus it does not require mechanism for either deployment or beam steering. The direct radiating phased-array antenna can achieve a wide beam-scanning range electronically. Electronic beam steering can be extremely agile, allowing virtually instantaneous beam repositioning from one direction to another. The generation of multiple independently steered beams from a single aperture is also possible. Because the beam is electronically steerable, no gimbaling is required, permitting agile beam repositioning at high rates. The challenges in phased arrays are that they are complex to implement, bulky and costly for high data-rate satellite communications and can require high dc power for all

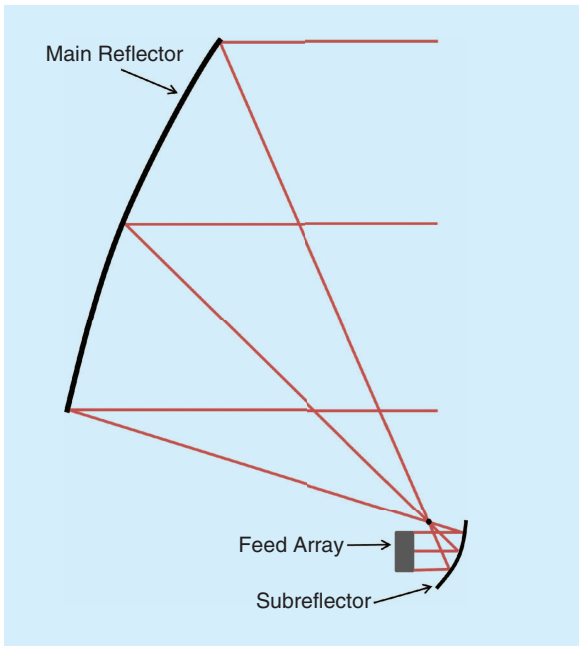


**Figure 8.** A phased-array fed imaging reflector antenna. The feed of the antenna is an array instead of a fixed antenna. Steering the beam of the feed array allows the beam of the full antenna to be steered (from [31]).

of the electronics. Progress had been made in advancing phased arrays for space applications, though the fundamental challenges remain.

A Ka-band active phased-array antenna has been developed at the National Institute of Information and Communications, Japan, for the Wideband Inter Networking Engineering Test and Demonstration Satellite (WINDS) [29]. It has a separate transmit and receive antenna, each of which consists of 128 radiating elements and high-density RF modules using GaAs MMICs that are attached to the elements. The element uses a pyramidal horn structure. The transmitting and receiving antenna can each electronically scan two independent beams. The antenna system is bulky, heavy, and complicated, having a size of  $1,510 \times 990 \times 1,530$  mm and a mass of 183 kg.

Harris developed a 20-GHz phased-array antenna for geosynchronous satellite communications [30]. The antenna array consists of 640 circularly polarized antenna elements. Each aperture is divided into RF sub-arrays consisting of 32 radiating elements, 32 element modules, and an integrated distribution and beam-forming network. The antenna is right-hand circular polarized, and can scan from bore-sight to  $9.3^\circ$ . The antenna has a size of  $1,117 \times 784 \times 226$  mm, and a mass of about 27 kg.

### Phased-Array Fed Reflector Antenna

An alternative to the traditional phased array is a phased-array-fed single reflector antenna which is superior in terms of reduced satellite payload mass; payload mass can be reduced by removing the subreflector and its

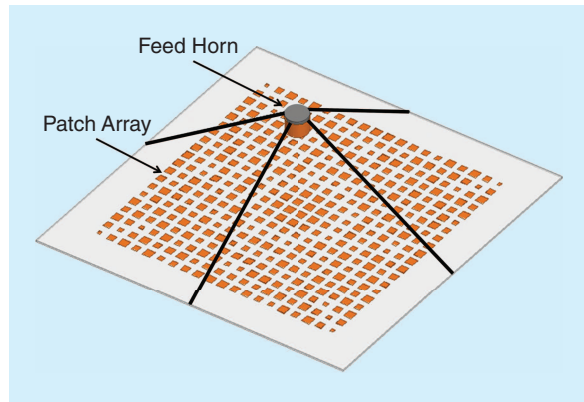


**Figure 9.** A planar reflectarray, which is fed by a horn antenna. The feed illuminates the reflect array, which retransmits as a formed beam. Each element controls the phase of its retransmitted signal, allowing for steering and beamforming like a traditional phased array.

tower, but scan loss generally increases when the beam is scanned widely.

The phased-array-fed imaging reflector antenna, which is composed of a main reflector and a subreflector, can obtain a performance equivalent to that of a large-scale direct radiating phased-array antenna. An example of a phased-array-fed imaging reflector antenna is shown in Figure 8. Precise beam pointing control can be realized by driving the subreflector. However, because the number of the radiating elements on the satellite should be as few as possible, grating lobes are generated if there are too few radiating elements.

A 20-GHz onboard phased-array-fed imaging reflector antenna has been developed by Nippon Telegraph and Telephone (NTT), Japan, for broadband satellite communications [31]. It achieves high gain and low grating lobes of 30 dB less than the peak gain, by controlling the distance between the array plane and the center of the subreflector. The antenna has a main reflector diameter of 3.5 m, and the focal length of the main reflector is 2.8 m.

### Reflectarray Antenna

A reflectarray antenna offers the possibility to reduce the cost and time for manufacturing the satellite antennas. It combines the advantages of printed microstrip technology and mature reflector technology. A feed illuminates a reflecting surface that has a locally controlled surface impedance to produce either a fixed or scanning radiation pattern [33]–[35]. The reflecting surface is a planar array where the power received by each element is reradiated with a prescribed phase to steer the beam [33]–[35]. An example of a reflectarray is shown in Figure 9.

For Direct Broadcast Satellite, a Ku-band 1-m reflectarray has been developed by Universidad Politécnic de Madrid (UPM), Spain [27]. It employs three layers of varying-sized patches and achieves a contoured beam. It

## To communicate with small mobile terminals on the ground, high equivalent isotropic radiated power (EIRP) and gain/noise temperature ratio (G/T) are required.

can fulfill the coverage of South America for both transmit and receive bands.

A dual-frequency X/Ka band reflectarray has been developed by Texas A&M University for NASA's future space communication applications [27]. It is circularly polarized and uses variable-angularly rotated annular rings. The antenna, with a diameter of 0.5 m, uses a multilayer technique in which the X-band annular rings are placed above the Ka-band rings.

A multifed and multibeam reflectarray has been designed in the 24.5–26.5-GHz band [34]. The antenna produces three independent beams in an alternate linear polarization that are shaped both in azimuth (sectored) and in elevation (squared cosecant). The design process is described in [34]. A breadboard has been manufactured and measured to validate the design process. The measured patterns are in close agreement with the simulations. These results show that several simultaneous shaped beams can be generated with reflectarray technology in a one feed per beam basis.

Some research on Ka-band microelectromechanical systems (MEMS)-based tunable reflectarray is ongoing at Thales Alenia Space [35]. In this reflectarray, the element consists of a slotted patch loaded by MEMS switches. The activation of MEMS switches in up and down positions permit the control of phase shift of the reflection coefficient in each element. When these phase-agile elements are arrayed, the beam can be electronically scanned. Initial results of a few elements show the beam can be scanned. A complete reflectarray has not been demonstrated yet. Some circularly polarized reflectarrays for satellite communications are presented in [32].

### Software-Defined Radio

SDR and cognitive radio (CR) are the technologies that promise more efficient approaches to truly generalized radios that are able to use whichever communications waveforms one desires. The flexibility inherent to these approaches is a strong enabler for the development and growth of SDR/CR technologies for hybrid communications terminals. These terminals allow a joint benefit from the advantages and capabilities of both terrestrial (high data rate and worldwide penetration) and satellite (large coverage and broadcasting capability) telecommunications, while offering the agility and configurability that characterizes a software-based solution. The features of these Internet-working systems are particularly relevant to cope with applications that require a rapid deployment of radio communications links with

a minimum user intervention. CR coupled with SDR also enables the ability to dynamically assign frequency allocations and efficiently use available bandwidth. SDR/CRs can also be leveraged to implement channelizers, which are key to adapting to changing market demands and effectively addressing a range of applications, including both broadband and narrow band applications. SDRs can be used to continuously look at channel use, data rates and power levels to optimize the assigned channels for best link performance for each end-user application. Achieving this may require changing the waveform (modulation scheme) dynamically to realize the best channel use.

Since SDR/CR systems rely heavily on software, there is a greater emphasis placed on the computational power of the digital signal processor, field-programmable gate array (FPGA), or embedded processor that lie at the core of the system. The feasibility of efficient and cost-effective payloads based on digital processors is highly dependent on a number of key areas, in particular, on the quality of RF analog data information that adjacent systems are capable of providing. Thus, it is vital to optimize the interfaces between the digital processor and analog/mixed-signal blocks through capable RF-to-digital conversion chains to achieve peak performance in mission critical applications.

The following sections will be focused on the RF front end and more specifically on the conversion between analog and digital domains for RF applications.

### Reconfigurable RF and MW SDR/CR Front Ends

In the last few years, digital technology has advanced dramatically, not only on the data conversion side but also in digital processing. This fact allows for significant variations in the way RF and microwave satellite systems are being designed. For instance, the ability to convert a signal directly at L-, S-, or even C-band can be seen as a large leap in capability allowing greater system flexibility and reduction in power consumption. This is because a multitude of other components in the frequency conversion stages can then be eliminated.

Still, there are a couple of inevitabilities on the design, characterization, and performance of the functional elements used in RF-to-digital, digital-to-RF, and digital processing units, which when achieved, would be seen as a significant step for the practical realization and subsequent market exploitation of software-based reconfigurable satellite payloads at higher frequency bands (C/X/Ku/Ka and above). However, a major bottleneck for the deployment of such demanding reconfigurable SDR/CR systems is the hardware needed to realize such agile satellite payloads. Since, in theory, SDR/CR transceivers are required to operate in any channel over a wide frequency range, this causes significant problems in a wide variety of RF components, such as the antenna, filter/duplexer, PA, as well as in the data itself.

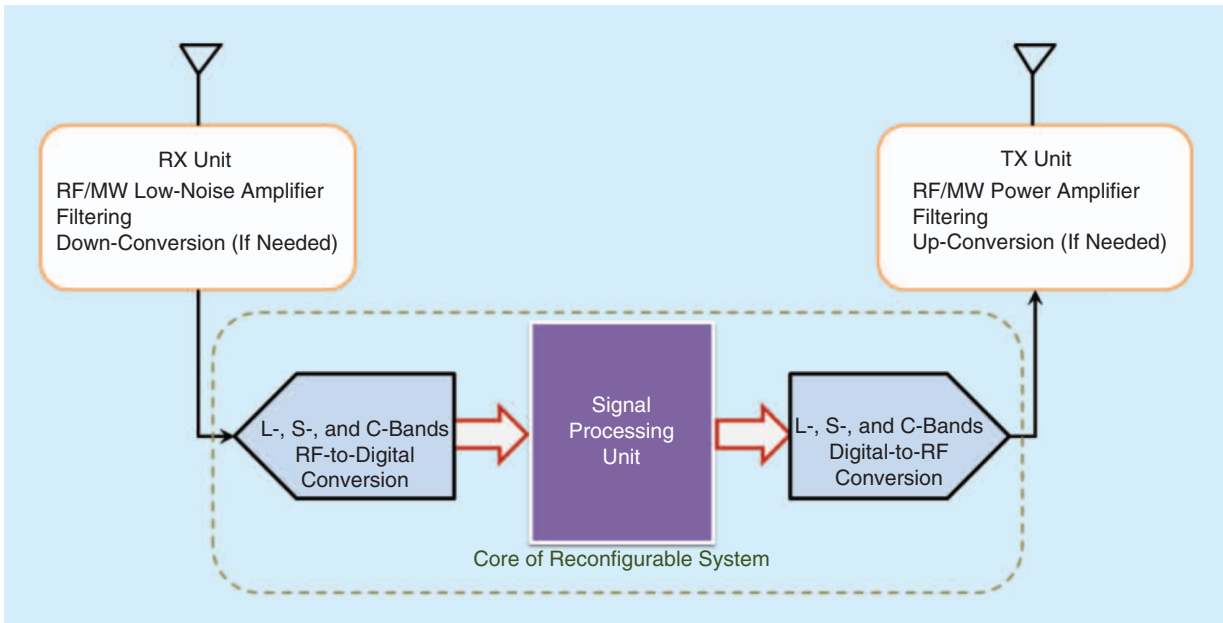


**Figure 10.** A generic block diagram for a reconfigurable SDR/CR transceiver for satellite applications.

In the area of RF-to-digital conversion, a number of techniques (like subsampling/band-pass sampling), with an associated elimination of the frequency conversion stage (or increase of the IF frequency), have been identified with a strong potential to improve performance and augment the level of integration of the analog preprocessor chains. In the area of digital-to-RF conversion, pulse-shaping, interpolation, and digital compensation can play a similar role for analog post-processor chains [37]–[39]. In the area of digital processors, there are a couple

of topics that are on the forefront of research activities, including channel switching, digital repeater schemes, and digital beamforming networks [40]–[42]. Within Europe, significant efforts have been made in the ESA, Centre National d’Etudes Spatiales (CNES), and European Commission (EC) programs on the hardware realization of high-speed broadband analog-to-digital converters (ADCs) and digital-to-analog converters (DACs) [37]–[40].

The future designs for reconfigurable satellite payloads would benefit much from the use of high capacity digital signal processors accompanied by resourceful and adaptable high-speed data conversion blocks.

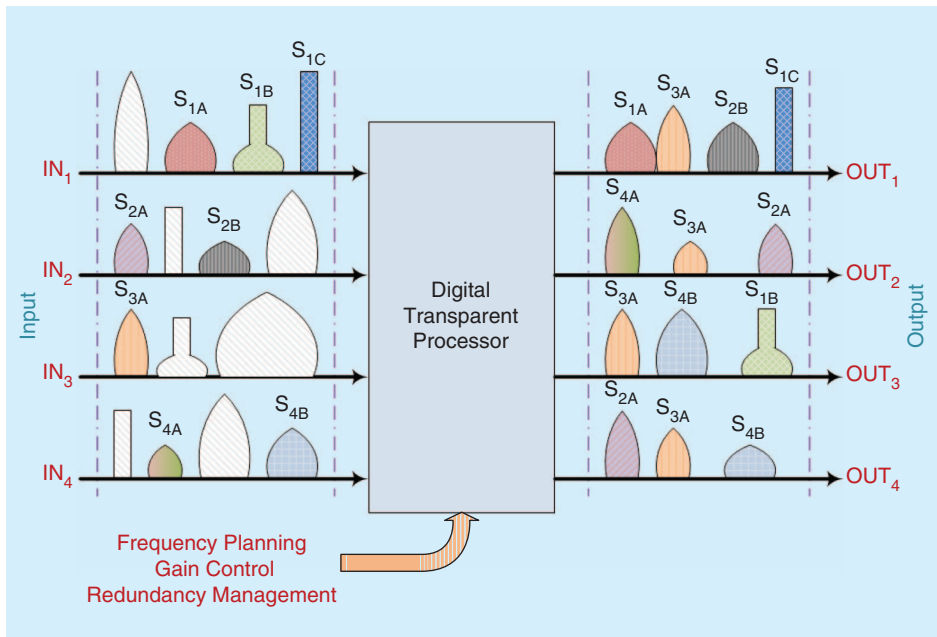


**Figure 11.** An illustration of digital processor functionality in a repeater having four inputs and four outputs, based on [40].

A generic block diagram accounting for this kind of reconfigurable SDR/CR transceiver scenario is sketched in Figure 10.

From Figure 10 it is noted that the removal of RF/IF frequency conversion stages and the ability to work directly at the lower GHz region opens the way for software defined reconfigurable microwave approaches in satellite payloads.

### High-Capacity Digital Processors

The heart of reconfigurable payloads is the digital processor, as it manages the connectivity by configuring

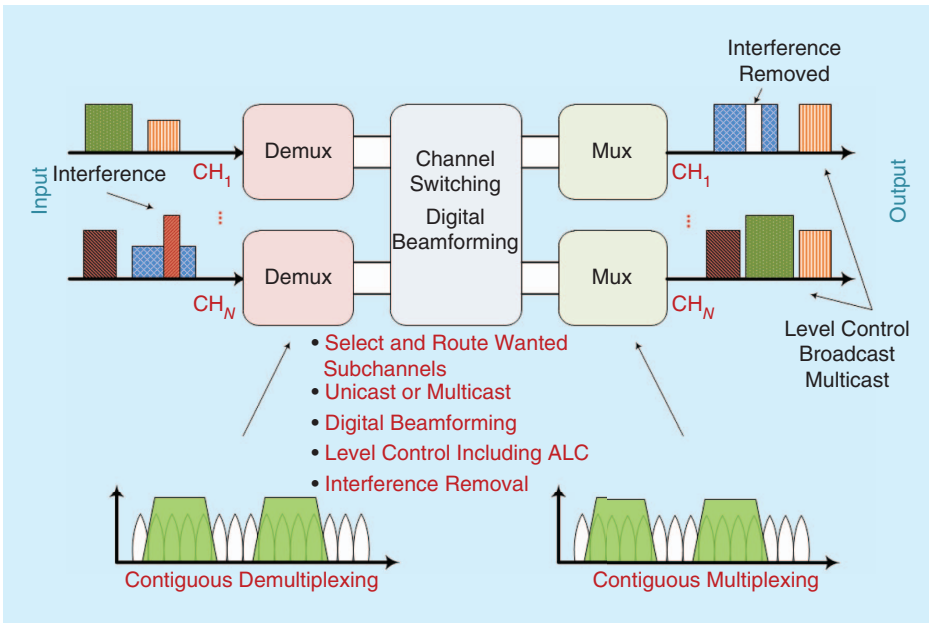


**Figure 12.** A functional block diagram of the next-generation processor developed by Astrium, based on [41].

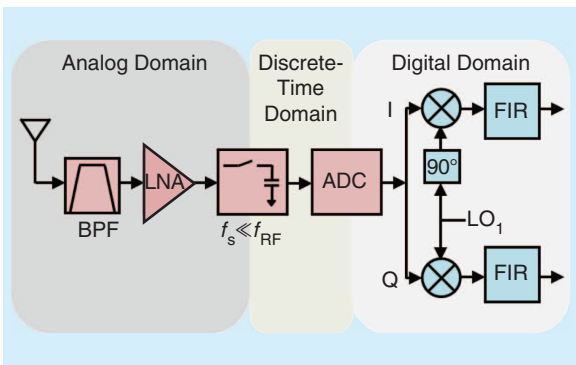


**Figure 13.** Bandpass sampling receiver simplified architecture, from [44].

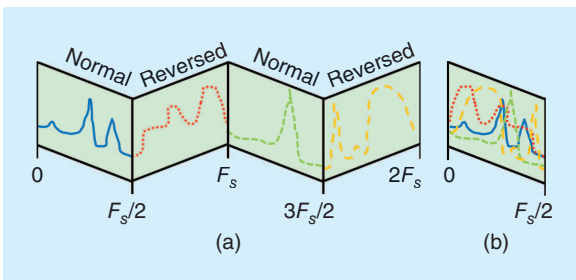


**Figure 14.** The process of folding that occurs in the sampler circuit, (a) input spectrum bandwidth, and (b) output showing the signals folded back into the first NZ, from [44].

the analog front ends and treating the data by adjusting the frequency operation of the channels. For example, Figure 11 shows a digital processor as the central part of a repeater system, in which it manages and processes the input and output channels by rearranging

the channel frequency and power levels [40].

Another example is the generic processor implemented by Astrium with strong support from ESA under the Next-Generation Processor program [41]. The outcome was a qualified processor that is compatible not only with the needs of narrowband mobile missions, but also much wider bandwidths as used in fixed service and broadband missions (as it is shown in Figure 12).

### Efficient RF-to-Digital Conversion

Efficient signal conversion from RF to digital

(usually having an ADC as core component) is crucial. This increased efficiency could be seen in the process of pushing the conversion domain as high in frequency as possible and to also capture the maximum available bandwidth, which will then provide an increased flexibility using digital signal processing. Some receiver solutions are supported in the bandpass sampling concept, which use an ADC that typically presents sampling rates lower than the RF signal carrier frequency. In this case, all of the energy from dc to the input analog bandwidth of the ADC will be folded back to the first Nyquist zone (NZ).

### Bandpass Sampling Operation

In the bandpass sampling receiver (BPSR) [43], shown in Figure 13, the incoming signal is initially filtered by an RF bandpass filter that can be a tunable filter or a bank of filters, and then amplified using a wideband low-noise amplifier (LNA). The signal is then converted to the digital domain by a high sampling rate ADC and digitally processed. Digital signal processing techniques can be used to alleviate some mismatches of the analog front end.

Thus, BPSR permits the implementation of an approach that allows all of the energy from dc to the input analog bandwidth of the ADC to be folded back to the first NZ [0,  $F_s/2$ ]. This process occurs without any mixing down-conversion because a sampling circuit is functionally replacing the mixer module. This is one of the most interesting components of this architecture, because it allows an RF signal of a higher frequency to be sampled by a much lower clock frequency. This process can be observed in Figure 14(a), in which we can see that all the input signals present in the allowable bandwidth of the sampling circuit

are folded back to the first NZ, Figure 14(b). As can be seen, the signals are down-converted and fall over each other if no filtering is used beforehand. This folding process occurs for all the available signals at the input of the circuit, including for any nonlinearity that may be present earlier (e.g., in the LNA) or even in the particular sampling circuit.

Obviously, a few critical requirements exist here, such as the fact that the analog input bandwidth of the sampling circuit must include the RF carrier band, and the clock jitter dependence must be accounted for, both of which can be serious problems in modern RF ADCs.

### Efficient Digital-to-RF Conversion

This section will address signal conversion from digital to RF (usually executed by a DAC), where a couple of designs that improve the performance of this function will be shown. In this area, pulse-shaping techniques [e.g., return-to-zero (RZ), non-return-to-zero (NRZ), etc.] and digital interpolation with oversampling DACs can play a similar role for the analog post-processor chains.

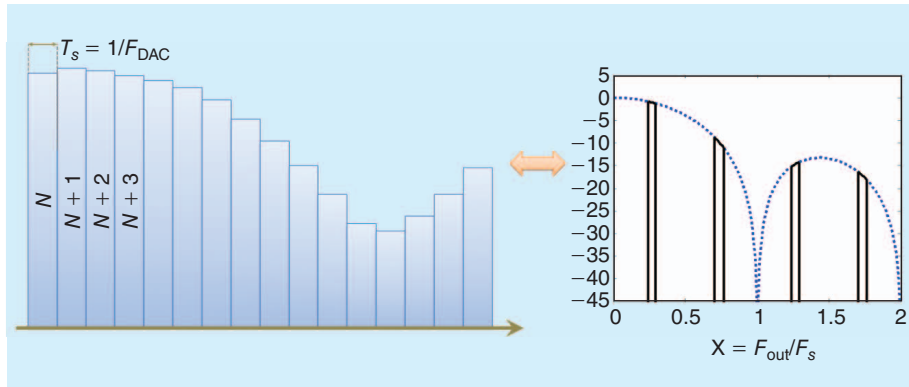


Figure 15. NRZ timing diagram and respective spectral representation.

### Digital-to-Analog Converter Operating Modes

Several operating modes are accessible in current RF DAC components, which rely on the reshaping of the analog DAC output level. The information provided in this section takes into account important capabilities offered on wideband DACs implemented under the ESA/CNES/EC High-Speed and Deep-Submicron microelectronics programs.

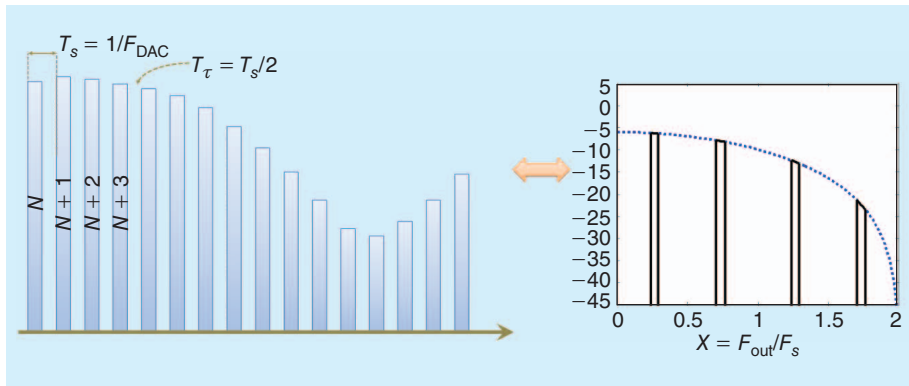


Figure 16. RZ timing diagram and respective spectral representation.

### Non-Return-to-Zero

This arrangement is the most common DAC working mode that is configured in any DAC with timing and spectral representation as shown in Figure 15. This mode does not allow for operation in the second and higher NZs because of the sinc(x) notch. The

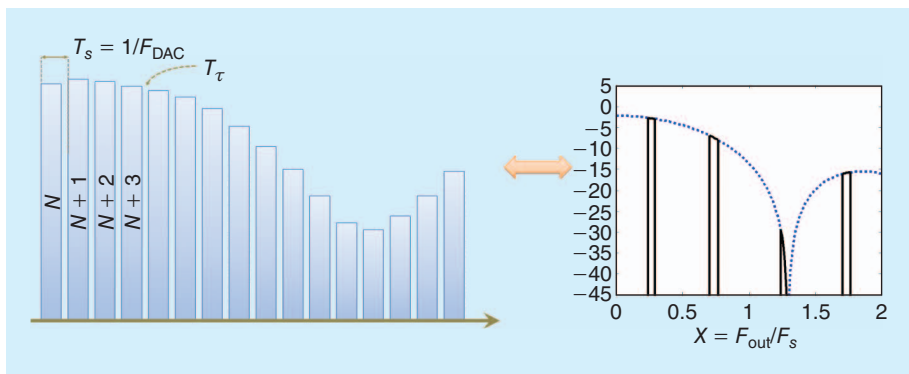


Figure 17. NRTZ timing diagram and respective spectral representation.

**This increased efficiency could be seen in the process of pushing the conversion domain as high in frequency as possible and to also capture the maximum available bandwidth, which will then provide an increased flexibility using digital signal processing.**

## The future designs for reconfigurable satellite payloads would benefit much from the use of high-capacity digital signal processors accompanied by resourceful and adaptable high-speed data conversion blocks.

advantage here is that it gives good results at the beginning of the first NZ (less attenuation than other architectures), and it removes the parasitic spur at the clock frequency (in differential mode)

$$P_{\text{NRZ}}(\omega) = 20 \log_{10} \left( \left| k \cdot \text{sinc} \left( k \cdot \pi \cdot \frac{\omega}{2} \right) \right| \right), \text{ where } k = 1. \quad (1)$$

### Return-to-Zero

In this structure, the shorter pulse (50% of the sampling period) results in reduced average amplitude imposing a degradation in the signal-to-noise ratio. The timing diagram and respective spectral representation for RZ format is shown in Figure 16. A shorter pulse changes the zeroth-order hold response dramatically as the first zero of the sinc(x) response is located at  $2 * F_s$ . This means that the frequency response of the DAC in the first NZ will be much flatter, thereby improving the step response of the DAC. The new response will show around 0.5-dB attenuation at  $F_s/2$ , whereas NRZ shows almost 4 dB of attenuation.

$$P_{\text{RZ}}(\omega) = 20 \log_{10} \left( \left| k \cdot \text{sinc} \left( k \cdot \pi \cdot \frac{\omega}{2} \right) \right| \right), \quad (2)$$

where  $k$  is the duty cycle of the clock presented at the DAC input (normally chosen as  $k = 1/2$ ).

### Narrow Return-to-Zero (NRTZ)

This mode offers optimum power over the full first NZ and the first half of the second NZ. The timing diagram for NRTZ is shown in Figure 17. It is recommended for best performance over the first and beginning of the second NZs, and has the following advantages:

- optimized power in first NZ
- extended dynamic range through elimination of noise on transition edges
- improved spectral purity
- trade-off between NRZ and RZ

$$P_{\text{NRTZ}}(\omega) = 20 \log_{10} \left( \left| k \cdot \text{sinc} \left( k \cdot \pi \cdot \frac{\omega}{2} \right) \right| \right),$$

where

$$k = \frac{\frac{1}{F_{\text{DAC}}} - T_{\tau}}{\frac{1}{F_{\text{DAC}}}}. \quad (3)$$

### RF or Doublet

This mode works like the NRTZ mode except for the polarity of one of the cores. The RF or Doublet timing diagram and associated spectral representation are shown in Figure 18. The inverted polarity can be accomplished by previously inverting the sample word applied to that core. Every sample will then consist of a doublet, where each half of the sample

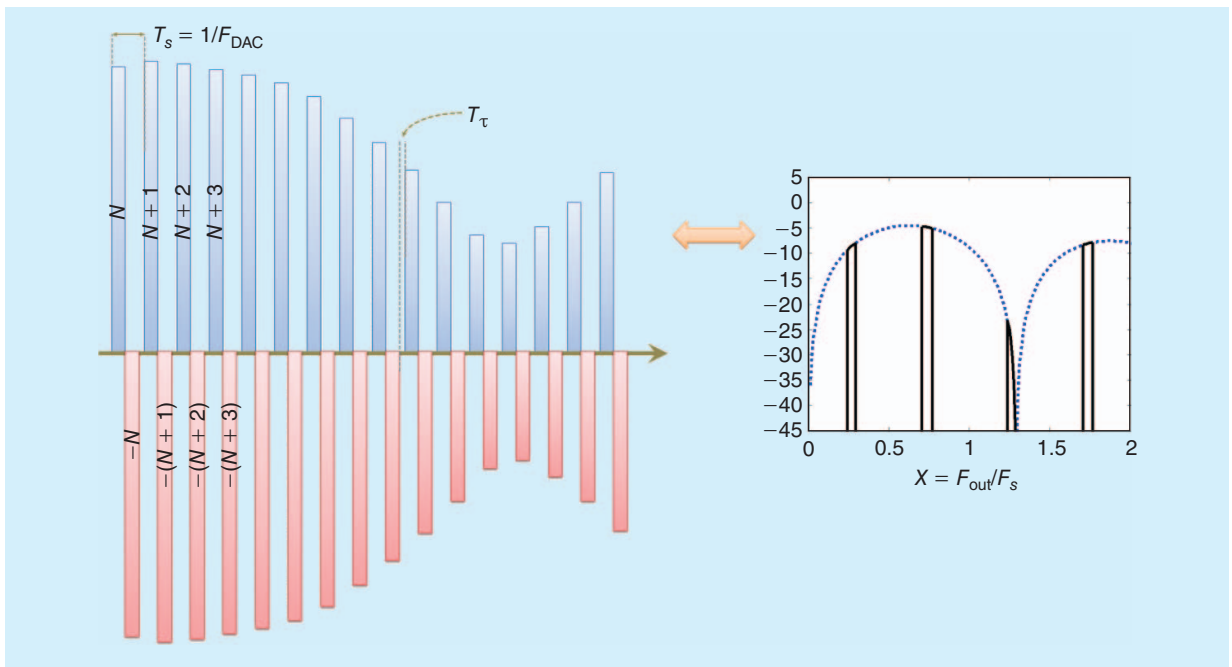


Figure 18. RF or doublet timing diagram and respective spectral representation.

time will be a RZ pulse with the same amplitude but inverse polarity. This mode presents a notch at dc and another notch that varies from  $F_s$  to  $2 * F_s$ , depending on the chosen resampling delay (represented in the equation by  $k$ ). Its minimum attenuation happens in this case at  $F_{out} = 0.78 * F_s$ , but in the case the reshaping pulse can be adjusted (defined in the equation by  $k$ ) it could present its minimum attenuation at frequencies that are closer to  $F_s$ . This response increases the amplitude of some high-frequency bands (second and third NZs), so it is especially useful when dealing with the generation of bandwidth-limited, high-frequency signals.

$$P_{RF}(\omega) = 20 \log_{10} \left( \left| k \cdot \sin c \left( k \cdot \pi \cdot \frac{\omega}{2} \right) \cdot \sin \left( k \cdot \pi \cdot \frac{\omega}{2} \right) \right| \right),$$

where

$$k = \frac{\frac{1}{F_{DAC}} - T_r}{\frac{1}{F_{DAC}}} \quad (4)$$

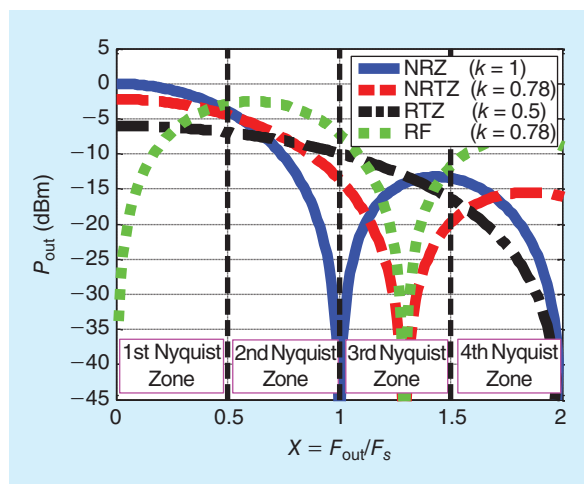


**Figure 19.** Frequency response of the different DAC working modes.

**Table 1. An outline of the major characteristics of each DAC operating mode.**

Operating Modes	Major Characteristics
NRZ	Maximum power in the first NZ and better performance in the beginning of the first NZ
RZ	Flatter response in the first and second NZs, having its first zero at $2 * F_s$
NRTZ	Best performance over first and beginning of second NZs and pushes images far away from $F_s$
RF	Increased performance for the second and third NZs and presents a notch at baseband

## The channelizer is used to distribute the total data capacity of the satellite across all of the beams it has for distribution.

### Performance Comparison of DAC Working Modes

In Figure 19, a general comparison is shown between the frequency responses of the different high speed DAC working modes. It is clear that very different shapes can be designed just by adjusting the ‘ $k$ ’ value, which is controlled in the resampling switch at the output of the DAC component. Table 1 summarizes the most important characteristics of each DAC operating mode by focusing on the individual power versus frequency responses.

### Conclusions

The increasing demand for broadband data continues across the full telecommunications industry, which includes satellite communications. This continued increasing demand along with rapidly changing markets is driving the key technologies in satellite communications. The key trends include increasing the bandwidths available along with the ability to adapt to changing market demands and changes in satellite fleets to distribute data efficiently across worldwide regions of coverage. This need for adaptability coupled with long satellite design lives is driving the demand for technologies that enable the satellite operators’ ability to redistribute the satellites capacity across coverage regions and markets and deployed satellites change. In the continued drive to more bandwidth, the industry moves toward higher frequency bands, beyond Ka-band, where more spectrum is available. Work is underway to understand the channel characteristics and mature technologies that can enable the use of those bands. This may include GaN, which offers the potential to deliver high solid-state power outputs with high reliability, though demonstrating this performance in real space environments is still ongoing. Technologies that can enable adaptability and greater flexibility in distributing broadband data across regions of coverage include new channelizers, phased-array antennas including array fed reflector antennas and reflectarrays in addition to SDRs. These technologies show great potential in allowing satellite operators the ability to quickly move coverage antenna beams, change allocations of a satellites total data capacity among beams, or to fundamentally change radio functionality, including waveforms after launch. Each of these technologies has continued to mature for nonspace applications and are showing great promise for space.

### References

- [1] Satellite Industry Association. (2012, Dec.). Satellites 101, Satellite Technology and Services. [Online]. Available: <http://www.sia.org>
- [2] Satellite Industry Association. (2012). State of the Industry Report. [Online]. Available: <http://www.sia.org>

- [3] 2012 *Playbook*, Telecommun. Ind. Assoc., Arlington, VA.
- [4] J. F. Reilly, II, "The space report," in "Space Foundation," Dean Sci. Technol., Amer. Public Univ., Charles Town, WV, Tech. Rep. 2013.
- [5] Viasat. [Online]. Available: <http://www.viasat.com/broadband-satellite-networks/high-capacity-satellite-system>
- [6] C. Wang, "Commercial satellite communications: Getting to Ka-band and moving beyond," in *Proc. IEEE Int. Microwave Symp. Workshop, Satcom Aerospace Beyond Ka-Band: Progress Challenges*, June 2013, pp. 1–26.
- [7] D. Gupta, "Prime: A market forecast for high-frequency, space-qualified, TWTs," *SatMagazine*, vol. 4, no. 12, pp. 52–65, Mar. 2012.
- [8] I. Verma and E. Wiswell, "Next generation broadband satellite communication systems," in *Proc. 20th AIAA Int. Communication Satellite Systems Conf.*, 2002.
- [9] M. Holmes. (2013, Feb.). Technology preview: Satellite 2013. Satellite Today. [Online]. Available: <http://www.satellitetoday.com/publications/2013/02/01/technology-preview-satellite-2013/>
- [10] Boeing company Web site. [Online]. Available: [http://www.boeing.com/boeing/defense-space/space/bss/factsheets/702/wgs/wgs\\_factsheet.page](http://www.boeing.com/boeing/defense-space/space/bss/factsheets/702/wgs/wgs_factsheet.page)
- [11] D. Runton, D. Aichele, M. LeFevre, and C. Burns, "Defining application spaces for high power GaN," in *Proc. IEEE MTT-S Int. Microwave Symp. Workshop, GaN for high power, High Bandwidth Applications: Finally Fulfilling the Promise*, 2010, pp. 1–27.
- [12] T. Ishida, "GaN HEMT technologies for space and radio applications," *Microw. J.*, vol. 54, no. 8, p. 56, 2011.
- [13] F. E. Nicol, B. J. Mangus, and J. R. Grebliunas, "TWTA versus SSPA: A comparison update of the Boeing satellite fleet on-orbit reliability," in *Proc. IEEE 14th Int. Vacuum Electronics Conf.*, 2013, pp. 169–170.
- [14] J. Cheron, M. Campovecchio, R. Quéré, D. Schwantuschke, R. Quay, and O. Ambacher, "High-efficiency power amplifier MMICs in 100 nm GaN technology at Ka-band frequencies," in *Proc. 8th European Microwave Integrated Circuits Conf. European Microwave Week, Nurnmberg, Germany*, 2013, pp. 492–495.
- [15] C. Campell, "A K-band 5 W Doherty amplifier MMIC utilizing 0.15 $\mu$ m GaN on SiC HEMT technology," in *Proc. Compound Semiconductor Integrated Circuit Symp.*, La Jolla, CA, 2012, pp. 1–4.
- [16] A. Brown, K. Brown, J. Chen, K. C. Hwang, N. Kolas, and R. Scott, "W-band GaN power amplifier MMICs," in *Proc. IEEE MTT-S Int. Microwave Symp. Dig.*, 2011, pp. 1–4.
- [17] P. Waltereit, J. Kühn, R. Quay, F. van Raay, M. Dammann, M. Cäsar, S. Müller, M. Mikulla, O. Ambacher, J. Lätti, M. Rostewitz, K. Hirche, and J. Däubler, "High efficiency X-band AlGaIn/GaN MMICs for space applications with lifetimes above 10<sup>5</sup> hours," in *Proc. 7th European Microwave Integrated Circuits Conf.*, Amsterdam, The Netherlands, Oct. 29–30, 2012, pp. 123–126.
- [18] R. Quay, P. Waltereit, J. Kühn, P. Brueckner, M. van Heijningen, P. Jukkala, K. Hirche, and O. Ambacher, "Submicron-AlGaIn/GaN MMICs for space applications," in *Proc. Int. Microwave Symp.*, Piscataway, NJ, 2013.
- [19] European Space Agency. (2013, May 3). *Proba-V Debuts New Semiconductor Technology for Space*. [Online]. Available: [http://www.esa.int/Our\\_Activities/Technology/Proba\\_Missions/Proba-V\\_debuts\\_new\\_semiconductor\\_technology\\_for\\_space](http://www.esa.int/Our_Activities/Technology/Proba_Missions/Proba-V_debuts_new_semiconductor_technology_for_space)
- [20] S. Colangeli, A. Bentini, W. Ciccognani, E. Limiti, and A. Nanni, "GaN-based robust low-noise amplifiers," *IEEE Trans. Electron Devices*, vol. 60, no. 10, pp. 3238–3248, Oct. 2013.
- [21] M. Rudolph, R. Behtash, R. Doerner, K. Hirche, W. Joachim, W. Heinrich, and G. Trankle, "Analysis of the survivability of GaN low-noise amplifiers," *IEEE Trans. Microwave Theory Tech.*, vol. 55, no. 1, pp. 37–43, Jan. 2007.
- [22] A. Jebri, M. Lucente, M. Ruggieri, and T. Rossi, "WAVE—A new satellite mission in W-band," in *Proc. IEEE Aerospace Conf.*, 2005, pp. 870–879.
- [23] M. Ruggieri, L. Vanni, L. Di Cecca, A. Salome, and M. Ruggieri, "The W-band data collection experiment of the DAVID mission," *IEEE Trans. Aerosp. Electron. Syst.*, vol. 38, no. 4, pp. 1377–1387, 2002.
- [24] BAA-RV-12-06 W/V-Band Communications Experiment. [Online]. Available: <https://www.fbo.gov/index?s=opportunity&mode=form&id=1042cca5bc2ca60e8f186bb1ce961bed&tab=core&cview=1>
- [25] A. Paoletta, "Space based communications at V & W Band: Characterization of atmospheric effects," in *Proc. IEEE Int. Microwave Symp. Workshop Satcom Aerospace Beyond Ka-Band: Progress Challenges*, June 2013, pp. 1–30.
- [26] A. J. Theiss, C. J. Meadows, R. Freeman, R. B. True, J. M. Martin, and K. L. Montgomery, "High-average-power W-band TWT development," *IEEE Trans. Plasma Sci.*, vol. 38, no. 6, pp. 1239–1243, 2010.
- [27] W. Imbriale, S. Gao, and L. Boccia, Eds., *Space Antenna Handbook*. Hoboken, NJ: Wiley, May 2012.
- [28] EADS Astrium. (2014, Jan. 15). [Online]. Available: <http://www.astrium.eads.net/en/homepage>
- [29] Y. Masanobu and T. Hasegawa, "Ka-band active phased-array antenna," Natl. Inst. Commun. Technol., Japan, Tech. Rep., Mar. 2006, vol. 54.
- [30] J. Warshowsky, C. Kulisan, and D. Vail, "20 GHz phased-array antenna for GEO satellite communications," in *Proc. IEEE AP-S*, June 2000, pp. 1187–1190.
- [31] S. Tanaka, S. Nakazawa, N. Kogou, K. Yamagata, and K. Shogen, "Onboard array-fed reflector antenna for 21-GHz-band direct broadcasting satellite," in *Proc. 1st European Conf. Antennas Propagation*, 2006, pp. 1–8.
- [32] Y. Imaizumi, Y. Suzuki, Y. Kawakami, and K. Araki, "A study on an onboard Ka-band phased-array-fed imaging reflector antenna," in *Proc. IEEE Antennas Propagation Society Int. Symp.*, San Antonio, TX, June 2002, pp. 144–147.
- [33] A. G. Roederer, "Reflectarray antennas," in *Proc. 3rd European Conf. Antennas Propagation*, Mar. 23–27, 2009, pp. 18–22.
- [34] J. Huang and J. A. Encinar, *Reflectarray Antennas*. Hoboken, NJ: Wiley, 2008.
- [35] H. Legy, Y. Cailloce, O. Vendier, G. Caille, J. Perruisseau-Carrier, M. Lathi, J. P. Polizzi, U. Oestermann, P. Pons, and N. Raveu, "Satellite antennas based on MEMS tunable reflectarrays," in *Proc. 2nd European Conference Antennas Propagation*, 2007, pp. 1–6.
- [36] S. Gao, Q. Luo, and F. Zhu, *Circularly Polarized Antennas*. Hoboken, NJ: Wiley-IEEE Press, Feb. 2014.
- [37] N. Chantier, F. Bore, M. Wingender, and A. Glascott-Jones, "Zero-IF, GHz bandwidths and software defined microwave approaches: Possibilities created by the latest data converter technology," in *Proc. 2nd ESA Workshop Advanced Flexible Telecom Payloads*, Noordwijk, The Netherlands, Apr. 2012, pp. 1–8.
- [38] L. Hili, P. Angeletti, and M. Nikulainen, "Overview of ESA developments on high-speed and deep sub-micron digital technologies," in *Proc. ESA Workshop Advanced Flexible Telecom Payloads*, Noordwijk, The Netherlands, Nov. 2008, pp. 1–4.
- [39] L. Hili, L. Dugoujon, P. Roche, F. Malou, and P. Perdu, "Deep sub-micron 65nm program Perspectives for the next generation satellites," in *Proc. 2nd ESA Workshop Advanced Flexible Telecom Payloads*, Noordwijk, The Netherlands, Apr. 2012.
- [40] H. Gachon, B. Delpuech, and P. Voisin, "Digital processor for telecommunication payload," in *Proc. 2nd ESA Workshop Advanced Flexible Telecom Payloads*, Noordwijk, The Netherlands, Apr. 2012.
- [41] P. Cornfield, A. Bishop, R. Masterton, and S. Weinberg, "A generic on-board digital processor suitable for multiple missions," in *Proc. 2nd ESA Workshop Advanced Flexible Telecom Payloads*, Noordwijk, The Netherlands, Apr. 2012.
- [42] S. Brown, D. Howe, R. Hughes, G. Chiassarini, D. Gianfelici, P. Altamura, and P. Angeletti, "Proof of concept of a high-throughput processor for broadband access networks," in *Proc. 15th Ka Broadband Communications Conf.*, Cagliari, Italy, Sept. 2009.
- [43] R. Vaughan, N. Scott, and D. White, "The theory of bandpass sampling," *IEEE Trans. Signal Processing*, vol. 39, no. 9, pp. 1973–1984, Sept. 1991.
- [44] P. M. Cruz and N. B. Carvalho, "Wideband behavioral model for nonlinear operation of bandpass sampling receivers," *IEEE Trans. Microwave Theory Tech.*, vol. 59, no. 4, pp. 1006–1015, Apr. 2011.

